GCAGS JOURNAL
A Publication of the Gulf Coast Association of Geological Societies
www.gcags.org

DIAGENETIC EVOLUTION AND ITS INFLUENCE ON PETROPHYSICAL PROPERTIES OF THE JURASSIC SMACKOVER FORMATION THROMBOLITE AND GRAINSTONE UNITS OF LITTLE CEDAR CREEK FIELD, ALABAMA

Sandra N. Tonietto[1,2] and Michael C. Pope[2]

[1]*Petrobras, Leopoldo Américo Miguez de Mello Research Center (CENPES), Rio de Janeiro, 21941598, Brazil*

[2]*Department of Geology and Geophysics, Texas A&M University, MS 3115, College Station, Texas 77843–3115, U.S.A.*

ABSTRACT

The ooid-oncoid-peloid grainstone and the microbial thrombolite reservoir facies of the Smackover Formation at Little Cedar Creek Field (LCCF), Alabama, U.S.A., have only a minor amount of dolomitization, and most of the depositional texture of these reservoir units is preserved, making LCCF a unique location to study facies distribution and diagenetic alteration of these reservoir facies. Depositional facies define good quality reservoirs in the Smackover Formation, but diagenesis plays an important role in enhancing or reducing their porosity and permeability.

The microbial thrombolite experienced the following early paragenetic sequence: (1) marine fibrous calcite rim cement, (2) early burial bladed to drusy calcite fringing cement, and (3) early burial mosaic calcite cement. The ooid-oncoid-peloid grainstone preserves a distinct early paragenetic sequence: (1) marine bladed calcite-rimming cement, (2) meteoric dissolution, (3) meteoric drusy calcite fringe cement, and (4) meteoric to early burial mosaic calcite cement. Both reservoir facies record similar late diagenetic evolution: (1) anhydrite cementation, (2) fracturing (closed or cemented), (3) chemical compaction (generating stylolites), (4) a second generation of fracturing (open microfractures), (5) burial dissolution, (6) local dolomitization, (7) late burial coarse mosaic to blocky calcite cement, (8) local quartz cementation, and (9) pyrite nucleation.

The ooid-oncoid-peloid grainstone can be subdivided in two sub-units: oolitic grainstone and peloid-oncoid grainstone. The lateral distribution of these two sub-units shows that the ooid grainstone prograded over the peloid-oncoid grainstone to the southeast. Porosity values in the ooid-oncoid-peloid grainstone vary from 5 to 32%, and the areas where the ooid grainstone dominates have the greatest porosity values (16 to 26% average). Permeability values are similar all over the ooid-oncoid-peloid grainstone reservoir, commonly between 1 and 10 md.

The largest pores of the thrombolite occur in areas where the microbial thrombolite is thicker, indicating that the dissolution process follows depositional features. Dolomitization occurs only in the south portion of the field. In the grainstone reservoir, dolomite occurs in a very small amount, usually less than 3%. In the thrombolite reservoir, dolomitization is more intense, locally affecting up to 30% of the rock. Dolomitization associated with dissolution significantly enhances permeability in this reservoir facies, from tens of md (usually 20 to 80 md) to hundreds of md (150 to 850 md). Blocky calcite cementation is more intense in the north portion of the reservoir, where dolomite is absent. Calcite cement can reach as much as 75% of the rock, significantly reducing porosity. As the reservoir dips southwest, this heterogeneous late burial calcite cement and dolomite distribution indicates that the deeper portion saw waters with a distinct chemistry, different than the shallower northeast portion of the reservoir.

Manuscript received April 9, 2013; revised manuscript received July 17, 2013; manuscript accepted July 17, 2013.

GCAGS Journal, v. 2 (2013), p. 68–84.

INTRODUCTION

Depositional facies define good quality reservoirs of Smackover Formation, but diagenesis plays an important role on enhancing or reducing their porosity and permeability. Thrombolite and ooid-oncoid-peloid grainstone are the most prolific

reservoir facies of the Smackover Formation (Benson and Mancini, 1999; Kopaska-Merkel and Mann, 1991; Mancini et al., 1991, 2006), whereas dolomitization and dissolution are the main diagenetic processes improving porosity and permeability (Benson and Mancini, 1999; Benson, 1988; Kopaska-Merkel and Mann, 1991; Mancini et al., 1991; Moore and Druckman, 1981; Prather, 1992a).

The grainstone and thrombolite units of the Smackover Formation at Little Cedar Creek Field (LCCF), Alabama, U.S.A. (Fig. 1), have only a minor amount of dolomitization, and most of the depositional texture of the reservoirs is preserved, making LCCF a unique location among all the Smackover Formation reservoirs to study facies distribution and diagenetic alteration. Smackover Formation grainstone and thrombolitic reservoir facies in all other fields are intensely dolomitized (Barret, 1986; Benson and Mancini, 1999; Mancini et al., 1991; Prather, 1992b) and most of the depositional characteristics of these rocks were obscured.

The LCCF initiated its production of oil (42–46 API gravity) in 1994 and oil and gas in 1995, presenting in 2013 a cumulative production of 20 million barrels of oil and condensate and 19 million cubic feet of gas. Since 2005, LCCF is the top oil-producing field in Alabama. A gas-injection secondary recovery project within the grainstone reservoir facies began, and production from wells surrounding the two injection sites has increased since the project was initiated. A similar recovery project is currently being considered for the thrombolite reservoir unit.

Comparing depositional textures, diagenetic events, including percentage of cement and dissolution, and petrophysical properties across both reservoirs, provides better understanding of heterogeneities in the reservoir facies and may influence future exploration and exploitation decisions. This paper discusses the relationship between the original depositional texture and the subsequent diagenetic alteration in both Smackover Formation reservoirs at LCCF, as well as lateral and vertical variation of facies, diagenesis and petrophysical properties of the reservoirs.

GEOLOGIC SETTING

The Gulf of Mexico is a passive margin consisting of a thick section of Mesozoic and Cenozoic sedimentary strata whose basic structural and stratigraphic framework was established during the Late Triassic and Jurassic (Salvador, 1987). Lithospheric extension occurred during the Early to Middle Jurassic as North America rifted from Africa followed by a long period of thermal subsidence (Driskill et al., 1988). The Upper Jurassic (Oxfordian) Smackover Formation was deposited during a major transgression during the formation of oceanic crust in the Gulf of Mexico and its thermal subsidence is due to cooling of the oceanic crust (Mancini et al., 1999; Nunn et al., 1984).

Seawater first inundated the Gulf of Mexico during the late Bathonian or the Callovian (Middle Jurassic) and was followed by a widespread and prolonged marine invasion during the Oxfordian. The shallow restricted hypersaline waters from which the Callovian salt precipitated were replaced during the Oxfordian by an increasingly larger and deeper water mass with unrestricted circulation and normal salinity (Salvador, 1987). The Upper Jurassic (Oxfordian) Smackover Formation records carbonate deposition on a carbonate ramp (Ahr, 1973). Local variations in topography on the ramp occurred due to the presence of a pre-Jurassic salient or were produced by salt tectonics (Ahr, 1973; Driskill et al., 1988).

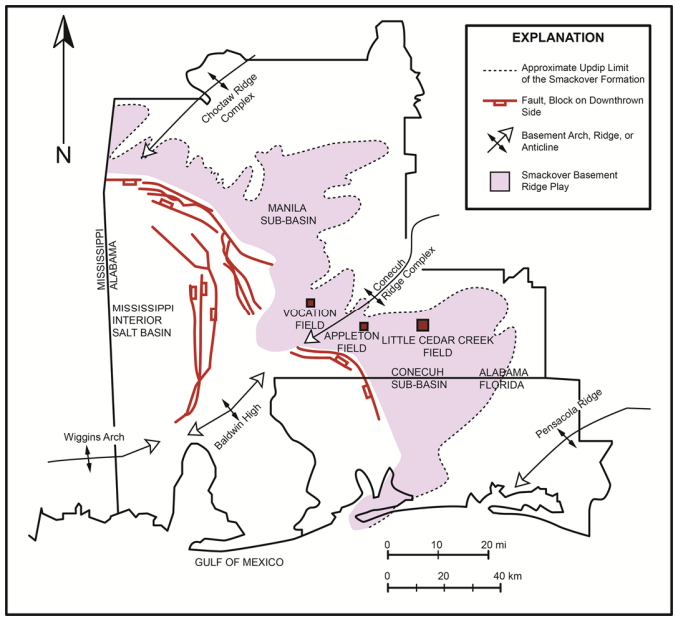

Figure 1. Location map of Conecuh Sub-basin and LCCF, southwestern Alabama, U.S.A. (modified after Mancini et al., 2008).

Conecuh Sub-Basin

Paleozoic ridges and Mesozoic horst blocks produced a number of paleohighs in the eastern Gulf of Mexico that separated southwest Alabama into a series of sub-basins or embayments (Benson, 1988; Mancini and Benson, 1980; Prather, 1992a). The Conecuh Ridge separates the Manila Sub-basin from the Conecuh Sub-basin, which is bordered to the southeast by the Pensacola Ridge (Fig. 1). The Wiggins Arch, an east-west trending basement high, borders the Mississippi Interior Salt Basin to the south and significantly influenced Smackover Formation deposition throughout much of southwest Alabama (Benson, 1988).

The Conecuh Sub-basin is located updip from the major rift-related fault trend (Fig. 1). The Smackover Formation in the Conecuh Sub-basin (as well as in the Manila Sub-basin) overlies continental crust extended by 25%, whereas the crust under the Smackover Formation updip, outside the embayments, corresponds to ~45% extension (Driskill et al. 1988). Landward from the peripheral fault zones, the magnitude of tectonic subsidence gradually increased from north to south. Basinward from the peripheral fault zones, magnitudes of the tectonic subsidence during the Jurassic and Cretaceous were nearly equal, but higher than in the landward direction from the peripheral fault zones (Driskill et al., 1988).

Sequence Stratigraphy

Upper Jurassic to Lower Cretaceous transgressive-regressive (T–R) sequences recognized in the Gulf of Mexico Coastal Plain record the post-rift tectonic and depositional history of this period. The Oxfordian was characterized by a widespread sea level rise that progressively affected larger parts of the Gulf of Mexico Basin and surrounding areas (Salvador, 1987). Four Upper Jurassic (Oxfordian) to Lower Cretaceous (Valanginian) T–R sequences occur across the Gulf Coast and the offshore northeastern Gulf of Mexico region (Mancini et al., 2008). The Smackover Formation sequence is subdivided into two systems tracts. The lower and middle Smackover Formation compose a transgressive systems tract (TST). Microbial reefs developed in the TST, and their growth ended before the maximum flooding zone (MFZ) that is characterized by a marine condensed section composed of relatively deep subtidal carbonate mudstone. The upper Smackover Formation (oncoid, peloid, and ooid grainstone to wackestone) and the Buckner Anhydrite Member of the Haynesville Formation represent a subsequent highstand systems tract (HST) (Mancini et al., 1990).

Smackover Formation Reefs

Reef growth was primarily described from the inner ramp areas, north of the Wiggins Arch (Parcell, 1999). Smackover Formation reefs occur from Arkansas to Florida as elongate features, 10 to 141 ft (3 to 43 m) thick, and several square kilometers in plan view. The reefs consist of cyanobacteria (microbial

buildups) or a more diverse coral-algal assemblage. Smackover Formation reef diversity is higher in southern Arkansas and northern Louisiana than in Alabama and Florida, where its depositional environment was more restricted (Baria et al., 1982). The reefs developed seaward of oolite shoals on three types of paleostructures that created subtle topographic highs: (1) basement ridges, (2) faulted basement highs, and (3) upthrown salt-cored fault blocks (Baria et al., 1982). However, LCCF microbial buildups developed in paleogeographic settings including nearshore, shallow subtidal paleoenvironments along the updip margin of the Smackover Formation rather than on Paleozoic basement paleohighs (Mancini et al., 2008).

Nearly all the microbial buildups in the eastern part of the trend (Alabama and Florida) formed at the base of the upper Smackover Formation, regardless of the structural setting of the reefs. However, in Alabama, reefs formed at the base of the lower Smackover Formation and also within the upper Smackover Formation, whereas in Arkansas and Louisiana, the reefs are stratigraphically higher, occurring only within the upper Smackover Formation. Microbial buildups generally form higher in the stratigraphic section in the downdip direction (Baria et al., 1982).

Smackover Formation Ooid-Oncoid-Peloid Grainstone to Packstone

Ooid-oncoid-peloid grainstone to packstone was deposited in the upper Smackover Formation during aggradation and progradation of shallow water shoal and tidal-flat complexes during a prolonged sea level highstand. The bulk of the upper Smackover interval consists of cyclic, coarsening upward sequences of peloidal, oncoidal, and oolitic packstone and grainstone. The uppermost cycles contain considerably more micrite than the lower cycles and fine rather than coarsen upward. In the Conecuh Embayment, peloidal and oncoidal grainstone and packstone interbedded with peloidal and skeletal packstone and wackestone predominate in the upper Smackover Formation. Oolitic grainstone is less common in this upper unit. Fauna are somewhat restricted and include abundant algal particles along with lesser numbers of foraminifera, ostracods, gastropods, and bivalves (Benson, 1988).

The grainstone facies in Alabama commonly consists of one or more upward shoaling cycles ranging from 15 to 50 ft (4.5 to 15 m) in thickness. These are 4th- or 5th-order cycles within the 3rd-order upper Norphlet to lower Haynesville depositional sequence (Kopaska-Merkel and Mann, 1993).

METHODS

Cores of 32 wells, consisting of 2610 ft (795 m) of rock, from LCCF were described using the Dunham (1962) classification of carbonate textures. Structures and macrotextures, porous intervals, and pore size were also documented. Samples include 192 plugs from cores (1-inch diameter) taken of a variety of textures and porosity features of the reservoirs. The wells analyzed occur across most of the field, and include both poor and highly productive wells. Log analysis, cross sections, and isopach maps were constructed with PETRA® software using the data of 77 wells (Appendix, Tables A–1 and A–2; Fig. 2A).

Standard petrographic analysis of 192 thin sections, 41 of which were stained with Alizarin Red-S and ferricyanide (Dickson, 1966) were used to characterize microfabrics, diagenetic features and porosity. Image analysis was performed on scanned thin section images (176 thin sections), and percentages of grains and porosity were quantified by IMAGO® software, resulting in a numerical estimative of cement in the microbial thrombolite reservoir (Appendix, Table A–1). Ten analyses were performed on each thin section to reduce analytical errors. Standard deviation from 0.9 to 8.1 was observed in the cement percentage values. Percentage of cement and grains were not calculated in the ooid-oncoid-peloid reservoir because of the poor contrast between them, so only their porosity was calculated.

Cathodoluminescence (CL) analysis was performed on all 192 thin sections, using a Technosyn cold cathode luminescence

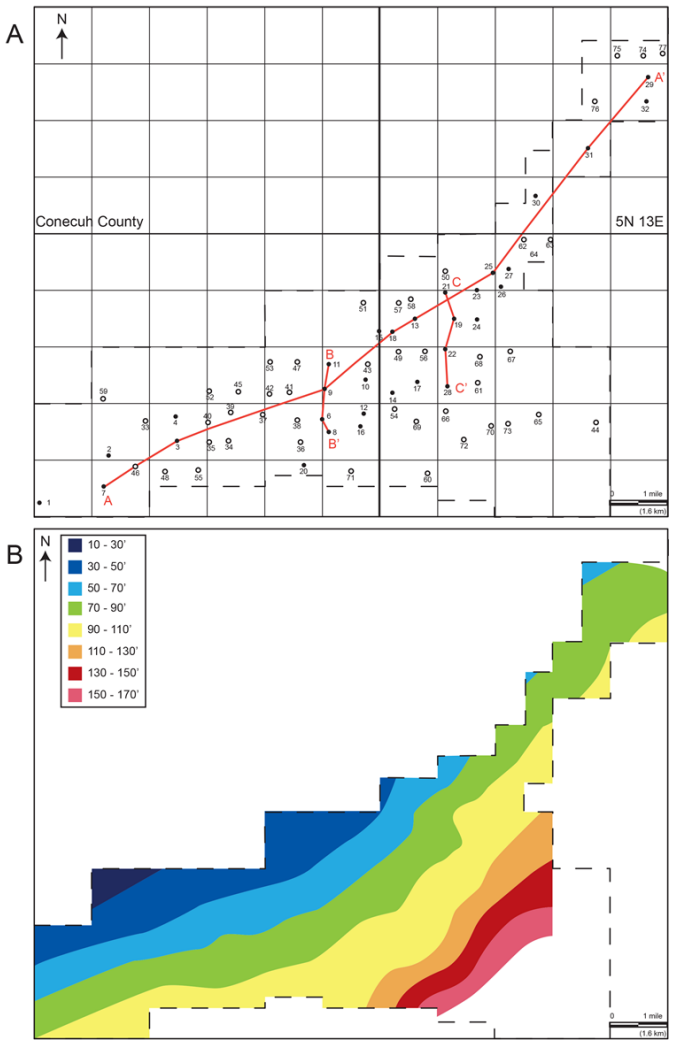

Figure 2. (A) Map of LCCF area with wells and cross section lines. See Figure 1 for regional location of the field. Wells depicted by black balls have logs, core description, and samples. Unfilled circles represent wells with logs, but without core description and samples. (B) Smackover Formation isopach map in Little Cedar Creek Field area showing thickening toward the southeast.

equipment, model 8200 MK II. Operating conditions for the analysis were 10 keV accelerating voltage and 300 µA current. The luminescence characteristics of the carbonate minerals are controlled primarily by the relative abundances of Mn, rare-earth elements (REEs), and Fe. The Mn^{2+} ion and trivalent REE ions (particularly Sm^{3+}, Dy^{3+}, and Tb^{3+}) appear to be the most important activator ions, whereas Fe^{2+} is the principal quencher (Marshall, 1988; Machel, 2000; Richter et al., 2003). Distinct luminescent zones based on the CL images were analyzed by microprobe to quantify Mn and Fe.

Trace-elements analyses of 187 data points in 12 selected thin sections were obtained using a four spectrometer Cameca SX50 Microprobe (Appendix, Tables A–3 and A–4). Operating conditions for the microprobe were 15 keV accelerating voltage, 50 nA beam current, and 10 µm spot size. Lower limit of detection (LLD) for each element in this condition are (ppm): Mn (130), Fe (150), Sr (290), S (60), Mg (60), and Na (80). The LLD is statistical, and is not necessarily a practical lower limit of determination. The error at the statistical LLD is infinite, thus the practical lower limit of determination is usually taken to be at least twice the statistical LLD (i.e., a concentration equivalent to at least six standard deviations of the background count

[Williams, 1987]). In the present work, only the values above twice the LLD (ppm) were used to calculate the average of each element (i.e., Mn [260], Fe [300], Sr [580], S [120], Mg [120], and Na [160]). Below these values the element was considered not detected or not present.

A paragenetic sequence based on petrography, cathodoluminescence, and minor and trace elements analysis was determined for each reservoir facies.

RESULTS

The Smackover Formation is 30 to 160 ft (9 to 49 m) thick in LCCF (Fig. 2B), where it comprises five units with distinct lithofacies and petrophysical characteristics (Figs. 3 and 4). From base to top, those units are: (1) microbial mats, (2) microbial thrombolite, (3) mudstone to peloid-oncoid packstone, (4) ooid-oncoid-peloid grainstone to packstone and (5) peloidal mudstone to wackestone, locally with very abundant siliciclastic grains. In the southwest portion of LCCF, a microbial thrombolite also locally occurs above unit 4 (present on well 20). The thicknesses of the five facies are different in each well, and some wells do not contain all the facies. In LCCF, only the microbial thrombolite and ooid-oncoid-peloid grainstone to packstone units are reservoirs, and they were described and analyzed in detail.

Microbial Thrombolite (Unit 2) and Ooid-Oncoid-Peloid Grainstone to Packstone (Unit 4) Reservoirs

The microbial thrombolite reservoir facies in LCCF is approximately 26 mi (42 km) long, 3 to 7 mi (5 to 11 km) wide, and from 30 to 70 ft (9 to 21 m) thick, and is elongated from northeast to southwest (Fig. 5A). It developed in a shallow subtidal environment not influenced by underlying basement topography (Koralegadara and Parcell, 2008; Mancini et al., 2006, 2008). The microbial thrombolite has a clotted, mottled and nodular texture, with rare domal and branching structures. The thrombolite includes abundant peloids, with minor amounts of skeletal fragments of benthic foraminifera and green algae (Fig. 6).

The ooid-oncoid-peloid grainstone to packstone reservoir in LCCF is approximately 18 mi (29 km) long, 5 to 7 mi (8 to 11 km) wide, and from 4 to 20 ft (1.2 to 6 m) thick (Fig. 5B). This facies is elongated in a northeast to southwest direction, mostly overlapping the microbial thrombolite unit. In the north portion of the field the ooid-oncoid-peloid grainstone to packstone unit is absent, replaced by a fine sandstone. The grainstone unit can be sub-divided into two subunits: ooid grainstone and peloid-oncoid grainstone to packstone (Fig. 7). Only the grainstone facies were described because porosity and permeability in the packstone intervals are very low or absent.

The ooid grainstone is composed by fine- to medium-sand-sized ooids (0.125 to 0.5 mm diameter) and a minor amount of coarse-sand to granule sized grapestones, bioclasts (mollusk, echinoid, benthic foraminifera, ostracods, and green algae), coarse to very coarse sand-sized oncolites and very fine to fine-sand sized peloids. The peloid-oncoid grainstone is composed of very fine to fine sand-sized peloids, coarse-sand to pebble-sized oncolites and a minor amount of bioclasts (mollusk, echinoid, benthic foraminifera, ostracods, and green algae) and ooids. Low to moderate bioturbation occurs in both sub-units.

The vertical distribution of the two grainstone sub-units changes in portions of the field. The facies distribution, when plotted in map view (Fig. 8) indicates that originally there were two main areas of ooid grainstone facies, almost isolated, which expanded laterally and prograded southeastward through time, forming a larger shoal, over the lower peloid-oncoid grainstone to packstone facies.

Paragenetic Sequence

The paragenetic relationships and geochemistry of the carbonate diagenetic components occurring in the Smackover Formation microbial thrombolite and ooid-oncoid-peloid grainstone to packstone units of LCCF are described to determine their diagenetic environments and evolution of the diagenesis.

The microbial thrombolite was deposited during a TST and was exposed only to marine waters during early diagenesis, but the ooid-oncoid-peloid grainstone was deposited during a HST (Benson, 1988; Mancini et al., 1990; Prather, 1992a) and also was exposed to meteoric phreatic waters.

The following paragenetic sequence characterizes the microbial thrombolite facies (in temporal order): marine fibrous calcite rim cement, marine to early burial bladed to drusy calcite fringing cement, early burial mosaic calcite cement, anhydrite replacement and cementation cross-cutting all previous phases, fractures (closed or cemented), chemical compaction, fractures (open microfractures), burial dissolution, dolomitization, late burial coarse mosaic to blocky calcite cement, and pyrite nucleation (Fig. 9A).

The ooid-oncoid-peloid grainstone facies underwent the following paragenetic sequence (in temporal order): marine bladed calcite rimming cement, meteoric dissolution, meteoric drusy calcite fringe cement, meteoric to early burial mosaic calcite cement, anhydrite replacement, fractures (closed or cemented), chemical compaction (generating stylolites), fractures (open microfractures), burial dissolution, dolomitization, late burial blocky calcite cement, and locally quartz cement (Fig. 9B).

Bladed calcite cement in the ooid-oncoid-peloid grainstone facies and fibrous calcite cement in the thrombolite facies formed within the marine environment. These cements form narrow crusts (usually less than 30 μm thick) rimming grains, and are non-luminescent.

After marine cementation, the ooid-oncoid-peloid grainstone was exposed to meteoric phreatic waters, which dissolved most of the oolites and precipitated a non-luminescent drusy calcite fringe cement and very fine mosaic calcite cement (Fig. 10). The drusy calcite fringe does not contain the trace-elements Fe, Sr, and Mn, and Na is low (318 ppm average) or absent. The absence of Mn causes the non-luminescent characteristic of this calcite cement phase. The low Na and the absence of Sr are indicative of a non-marine environment. Moldic and intragranular porosity was generated during this phase, whereas depositional intergranular porosity was partially or locally entirely obliterated. In the peloid-oncoid grainstone sub-unit, dissolution of the grains is less intense and intergranular porosity dominates, whereas in the oolitic grainstone the moldic porosity predominates.

In the microbial thrombolite reservoir facies, marine to early burial bladed to drusy calcite fringe cement rims peloid clusters and constructional voids (Fig. 11). This cementation phase has three distinct luminescent zones, from the center to the edge: zone 1, dull brown to nonluminescent; zone 2, light brown luminescence; and zone 3, orange luminescence. Generally in the smaller primary pores only the first or first and second zones developed. Increasing luminescence from the center to the edge of the cement records increasing amount of Mn (Figs. 12A and 12B) as a result of a continued growth of the meteoric drusy calcite fringe with burial. This shallow-burial phase of bladed to drusy calcite cementation also occurs in the grainstone reservoir facies.

Early burial mosaic calcite cement was precipitated after the bladed to drusy calcite fringe cement, and its luminescence is similar to that of zones 2 and 3 of the bladed to drusy calcite cement (i.e., dark to light brown and orange luminescence) but its crystals are larger, and do not rim the grains or peloid clusters. Mn content is similar to slightly higher than in the bladed to drusy calcite cement.

An uncommon characteristic of the meteoric mosaic calcite cement in the grainstone unit of LCCF is its high Sr content, with an average of 4121 ppm (as much as 6796 ppm). The meteoric mosaic calcite cement was precipitated by interstitial waters rich in Sr, which are interpreted as being derived from dissolved aragonitic oolites. High Sr content is unusual in ancient limestones, which show a median concentration of 400 to 700 ppm (Kinsman, 1969), although values range widely. High Sr content is common in aragonite (3000 to 10,000 ppm) and also occurs in calcite cements that formed by alteration or dissolution of aragonite (Budd and Land, 1990; Khale, 1965; Singh, 1987). The diagenetic alteration of typical aragonitic sediments can produce calcite with 700 to 10,000 ppm of Sr (Kinsman, 1969), and the

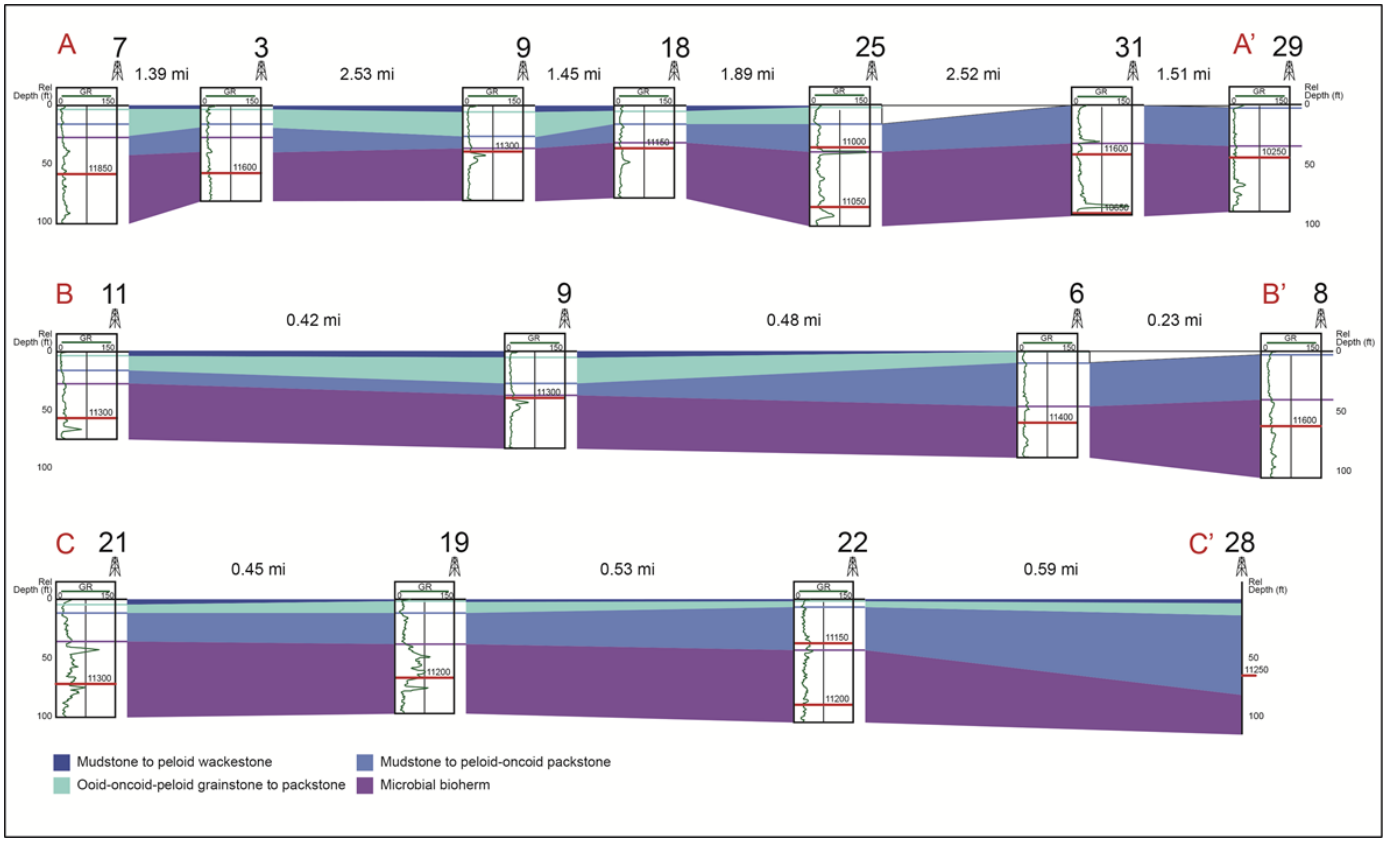

Figure 3. Stratigraphic cross sections of the Smackover Formation showing field-wide extent of depositional facies. (A) Strike cross section A–A′ oriented southwest to northeast. (B and C) Dip cross sections B–B′ and C–C′ oriented northwest to southeast. See Figure 2A for location of cross sections. Datum is top of Smackover Formation.

mosaic calcite cement in the grainstone unit of LCCF is interpreted to be an example of this process.

Due to early cementation, there is little or no evidence of grain compaction in either reservoir facies. However, deep burial compaction features, such as stylolites and solution seams, are abundant in both reservoir facies. Subvertical, inclined, and subhorizontal fractures are common, but their frequency is variable from approximately every 2 ft (60 cm) or 4 ft (120 cm), to approximately every 25 ft (7.6 m). All of the macroscopic fractures are closed or cemented by calcite, and most of them are discontinuous. Several fractures are crosscut by stylolites, indicating that this first fracturing event occurred before pressure dissolution caused by compaction. A second fracturing event produced open microfractures that crosscut stylolites and blocky calcite. A post-compaction dissolution event produced enlargement of primary depositional constructed vugs, and this process was more intense closer to major fractures.

Anhydrite cement occurs as millimeter-diameter patches that occlude pore space and replace grains and older calcite cements. It occurs in both reservoir facies but in very small amounts (commonly less than 1%). Dolomite forms as a replacing and cementing mineral, with euhedral to subhedral crystal shapes and red luminescence. Fe content varies from one dolomite crystal to another and throughout the same crystal (Fig. 12C). Locally, Fe content increases from center to border (dull luminescent border—zoned crystals); elsewhere it decreases toward the border (unzoned crystals). In general, dolomite is rare in the ooid-oncoid-peloid grainstone, commonly less than 3% of volume, and replace portions of grains. In the microbial thrombolite reservoir facies, dolomite is more abundant, composing as much as 30% of the rock and gradually decreasing from south to north in LCCF. It is absent from the center to the northeast portion of LCCF (Fig. 13A). The dolomite preferentially replaces the bladed to drusy calcite fringe cement, but it also replaces depositional grains and other cements. It is common for dissolution of calcite to be associated with dolomitization. Microprobe analysis shows that Sr, S, and Na are absent in most of the dolomite crystals (or occur in a very small amount, close to the lower limit of detection), indicating the dolomitizing fluid was not marine, and together with crosscuting relationships, supports its interpretation as a late burial dolomitization.

Late-burial, coarse mosaic to blocky calcite cement occurs in both reservoirs, but it is more abundant in the microbial thrombolite reservoir facies. The crystals commonly are zoned, with two to five luminescent zones, but some crystals are unzoned. The order of the luminescent zones is variable, with dark brown, light brown, orange, and light orange colors visible. Trace-element analyses shows that Sr and Na are absent, and Fe and Mn content are higher than in the bladed to drusy calcite fringe cement. In the microbial thrombolite facies the amount of coarse mosaic to blocky calcite increases to the north, where calcite cements compose more than 70% of the rock (Fig. 13B). Quartz cement (overgrowth) occurs only in the grainstone reservoir and is a localized diagenetic phase. Pyrite and galena are common accessory minerals in the thrombolite reservoir across the field.

Petrophysical Properties

The pore types in the microbial thrombolite are depositional constructional voids, vugs, intercrystalline porosity (when dolomitized) and microfractures. Most of the vugs were created by enlargement (dissolution) of constructional voids formed during microbial thrombolite development. Petrophysical characteristics are highly variable laterally and vertically inside the microbial thrombolite. The thickness of the microbial thrombolite increases from west (protected side) to east (greater paleoenvironmental energy), and the lateral pore size distribution follows the same trend, increasing from mesopores near the west border to mega-

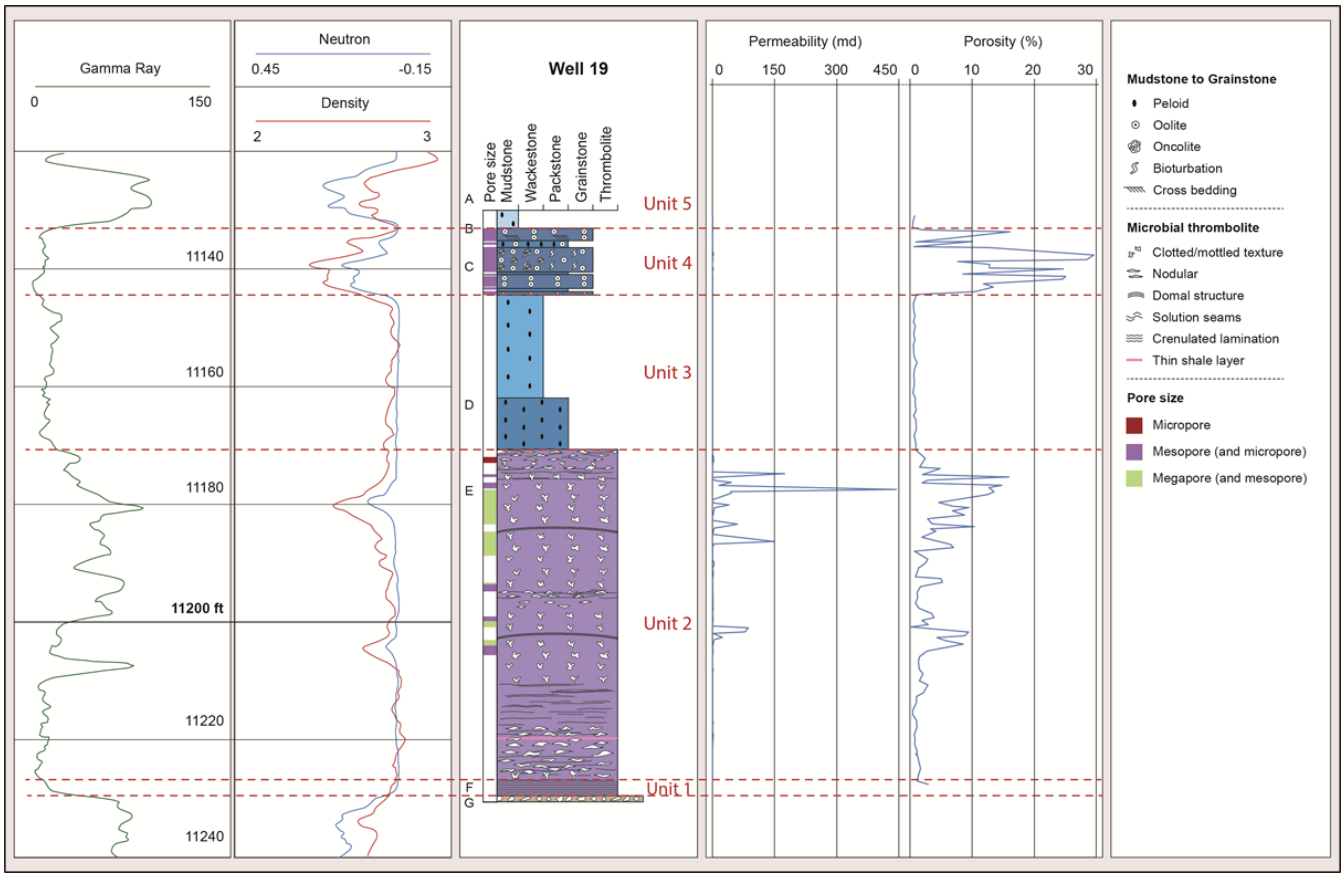

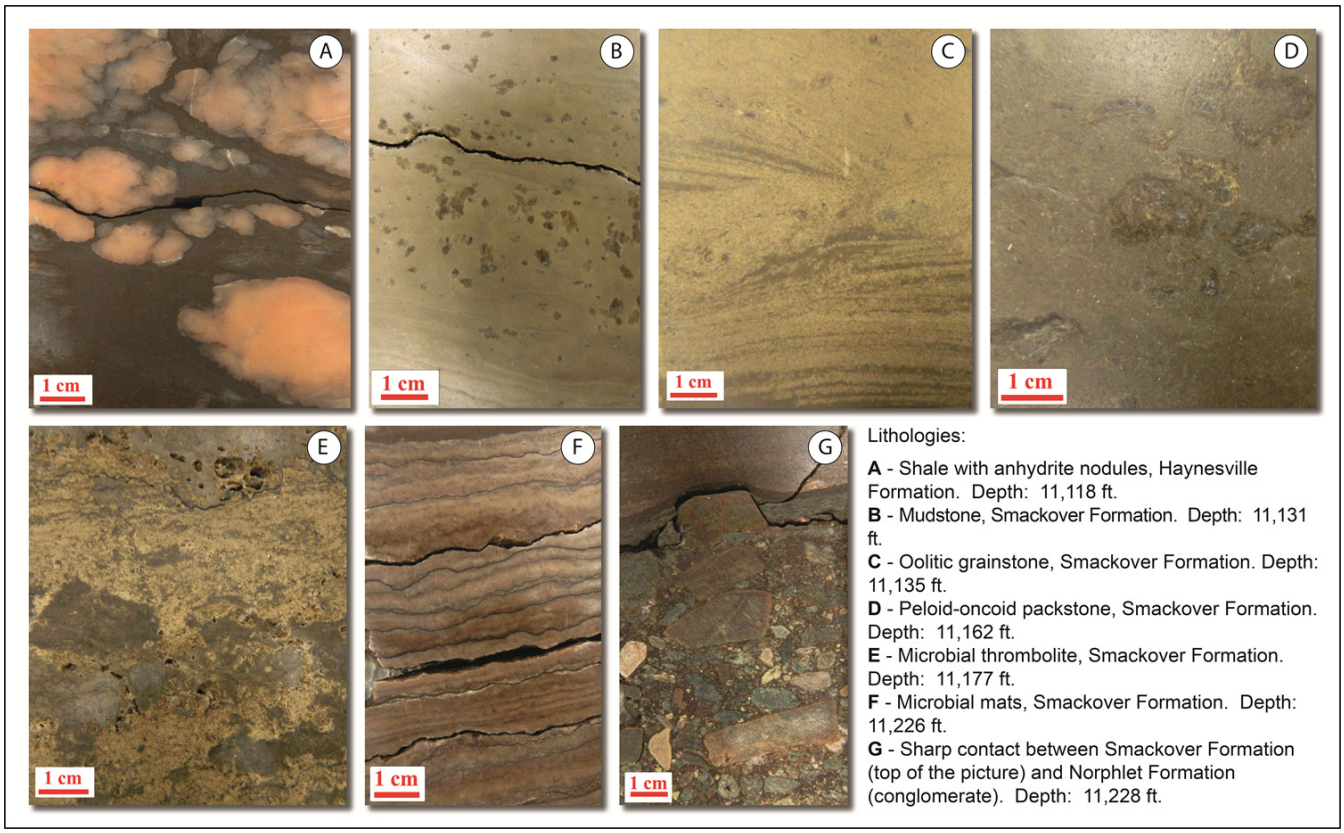

Figure 4. (A) Type log of Smackover Formation, well 19, Conecuh County, including gamma ray, neutron porosity, and density tracks, core description, porosity and permeability, and petrophysical analysis (plugs from cores). Units 1 through 5 are the (1) microbial mats, (2) microbial thrombolite, (3) mudstone to peloid-oncoid packstone, (4) ooid-oncoid-peloid grainstone to packstone, and (5) peloidal mudstone to wackestone facies. See Figure 2A for well location. (B) Core photos of lithologies in well 19. The location of the samples in the core is shown on Figure 4A.

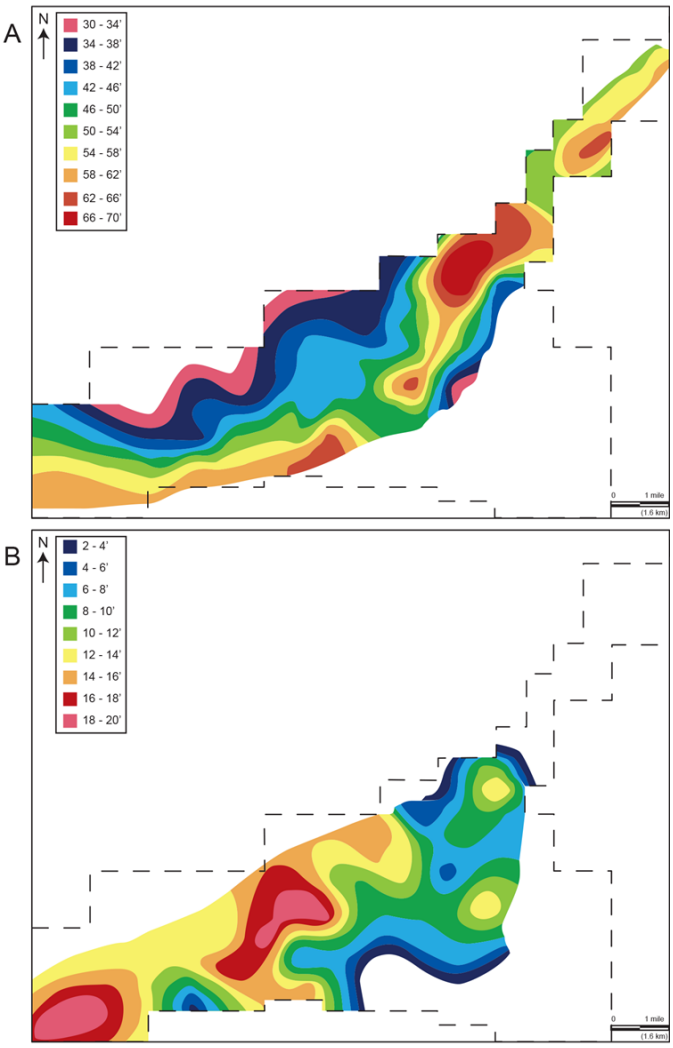

Figure 5. (A) Isopach map of microbial thrombolite facies in LCCF. (B) Isopach map of ooid-oncoid-peloid facies in LCCF. See Figure 2A for map location.

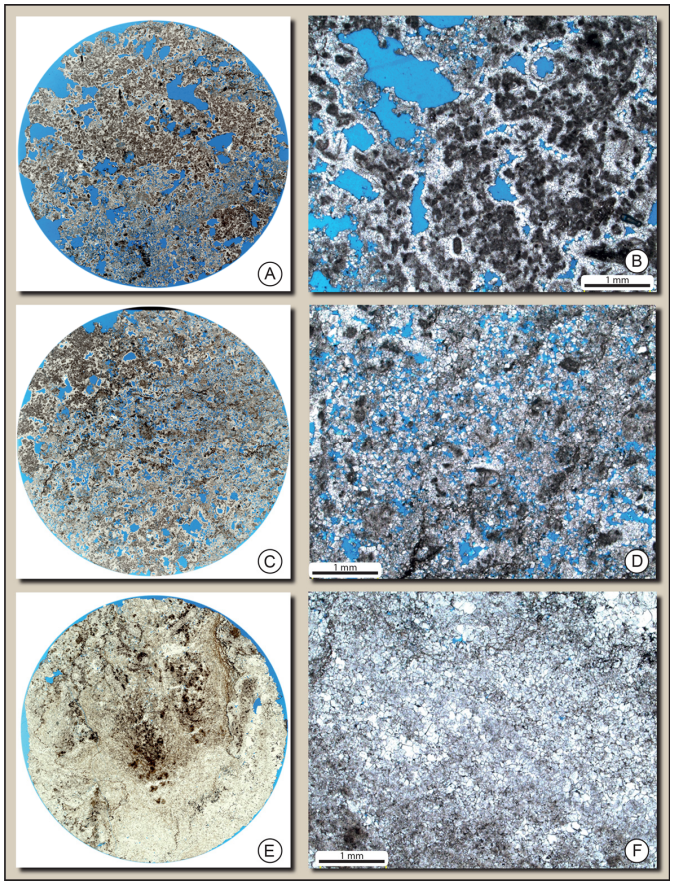

Figure 6. Paired images of scanned thin section of the thrombolite reservoir facies from 1 in (2.5 cm) diameter plugs (A, C, and E) and photomicrographs from the plugs (D, E, and F). (A and B) Microbial thrombolite. Peloids are the main constituent of the rock, being rimmed by calcite cement. Porosity, 21%; and permeability, 2.5 darcys. Well 3—depth, 11,609.5 ft. (C and D) Intensely dolomitized microbial thrombolite. Original peloidal texture was replaced by fine to very fine dolomite crystals. Porosity, 21%; and permeability, 370 md. Well 2—depth, 11,787.9 ft. (E and F) Microbial thrombolite extensively cemented by coarse mosaic and blocky calcite. Porosity, 1%; and permeability, <1 md. Well 17—depth, 11283.8 ft.

pores near the east border (Fig. 13C) where dissolution produced vugs from 0.8 to 2.4 in (2 to 6 cm) in diameter. In nondolomitized thrombolite, core-plug analysis shows that porosity values vary from 3 to 19% (Fig. 14A), and permeability values commonly vary from less than 1 to 100 md but locally are as much as 500 md where late dissolution is more intense. In partially dolomitized intervals of the thrombolite, porosity varies from 10 to 21%, and permeability varies from 150 to 850 md, locally as much as 1200 md (Fig. 14B). Large vugs and fractures cause local permeability values to be 1 to 4 darcys, and rarely as much as 7 darcys.

The ooid-oncoid-peloid grainstone has intergranular, intragranular, moldic and vuggy porosity. Microfractures are rare in this facies. The largest porosity values are associated with intense dissolution of the oolites, and consequently to the presence of moldic porosity. Porosity values vary from 5 to 32% (Fig. 15A), and the areas where the ooid grainstone is thicker have the greatest porosity values (16 to 26% average). The rimming calcite cements obstruct pore throats; therefore, permeability in the ooid-oncoid-peloid grainstone is low, commonly between 1 and 10 md, and has only small variations across the reservoir (Fig. 15B). Depositional intergranular porosity is more abundant where grains are coarser (medium to very coarse sand size) and cementation did not completely fill pore space. Locally, where vuggy porosity is abundant, permeability ranges from 100 to 500 md.

DISCUSSION

Early diagenesis of the Smackover Formation grainstone was regionally variable and was driven by meteoric waters to mixed and marine waters (Ahr and Palko, 1981; Benson and Mancini, 1999; Llinas, 2002; Moore and Druckman, 1981). The ooid-oncoid-peloid grainstone unit in LCCF is characterized by an early diagenetic phase similar to that of the Smackover Formation oolitic grainstone in Midway Field (southwest Arkansas) and Lincoln Parish (Louisiana), where early diagenesis was dominated by meteoric events (Ahr and Palko, 1981; Moore and Druckman, 1981). In these areas, the ooid grainstone is dominated by precompaction diagenetic fabrics, an absence of compactional features, and abundant moldic porosity, with little preserved depositional intergranular porosity. Original intergranular porosity commonly was filled with mosaic calcite cement. However, burial diagenesis varied between LCCF and Midway fields. In Midway field, the only late burial event was the local replacement by massive anhydrite laths that crosscut molds as well as cements (Moore and Druckman, 1981). The grainstone unit in LCCF underwent anhydrite replacement and several other burial events, such as chemical compaction, fracturing, late burial blocky calcite cementation, late burial dissolution and locally

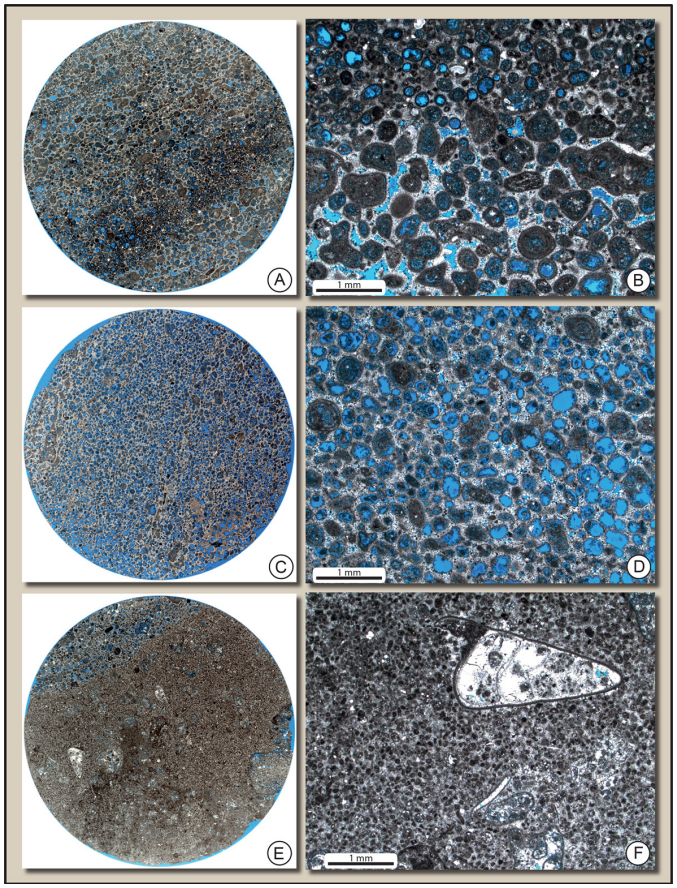

Figure 7. Paired images of scanned thin section of the ooid-oncoid-peloid reservoir facies from 1 in (2.54 cm) diameter plugs (A, C, and E) and photomicrographs of thin sections from core plugs (B, D, and F). (A and B) Ooid grainstone with fringing calcite cement. Porosity, 20%; and permeability, 6 md. Well 4—depth, 11,506 ft. (C and D) Ooid grainstone with oomoldic porosity. Porosity, 30%; and permeability, 0.7 md. Well 21—depth, 11,223.3 ft. (E and F) peloid-oncoid grainstone with bioclasts. Porosity, 3%; and permeability, 1.6 md. Well 15—depth, 11,266.5 ft.

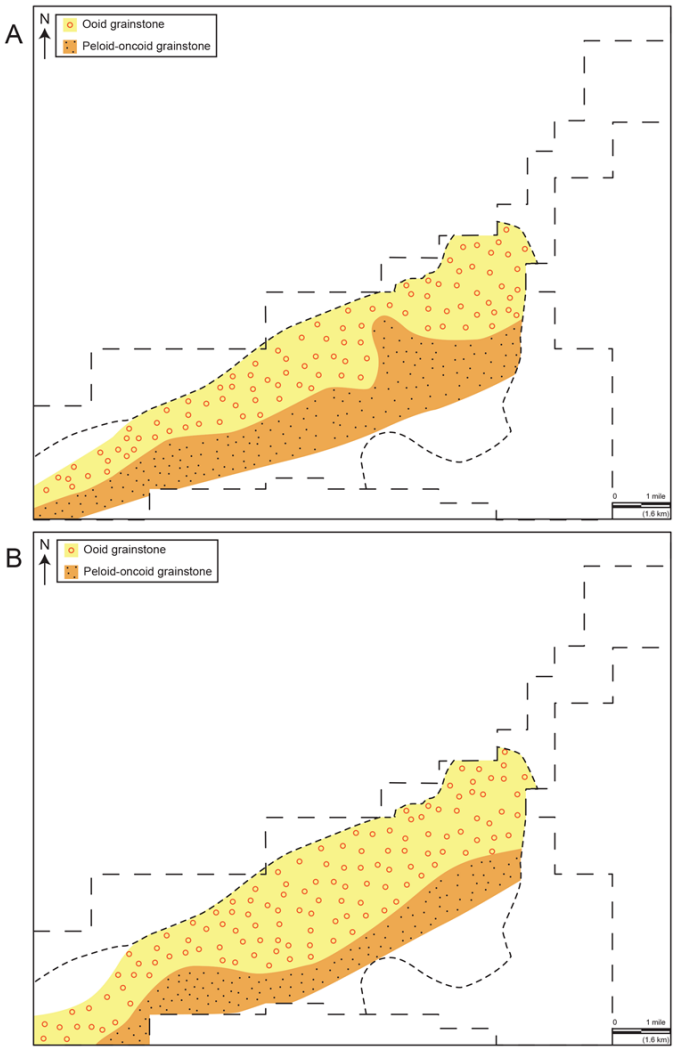

Figure 8. (A) Facies map of the base of the ooid-oncoid-peloid grainstone unit. (B) Facies map of the top of the ooid-oncoid-peloid grainstone unit. See Figure 2A for map location.

dolomitization. The diagenetic phases of the microbial thrombolite facies in LCCF cannot be compared with similar ones in other fields because all other Smackover Formation microbial thrombolite reservoirs studied are intensely or totally dolomitized, with no depositional microtexture, primary porosity features and pre-dolomitization diagenetic features preserved (e.g., Llinas, 2002; Petta and Rapp, 1990).

Both Smackover Formation reservoirs in LCCF record distinct early diagenetic phases, but both facies underwent a similar burial diagenetic evolution. Diagenesis significantly affected the pore system in both reservoirs. In the ooid-oncoid-peloid grainstone facies, marine cementation initiated lithification, but subsequent meteoric diagenesis modified the pore system. Its interconnected depositional intergranular pore system was transformed into an unconnected moldic, vuggy, and intragranular pore system by diagenesis. Meteoric drusy calcite fringe cement caused significant reduction of primary intergranular porosity, and pore throats were blocked. Meteoric dissolution formed secondary oolite molds that enhanced porosity but not permeability.

The early-burial, bladed to drusy calcite cementation phase formed in both the microbial thrombolite and ooid-oncoid-peloid reservoir facies. The marine and early burial calcite cements have uniform cathodoluminescence patterns across both reservoir facies, indicating uniform pore-water chemistry during cementation. However, later diagenetic phases formed in non-uniform ways within the reservoir facies, producing significant variation in the porosity and permeability of each reservoir.

During late burial diagenesis, vuggy porosity formed and locally enhanced permeability. Late calcite cementation did not significantly alter porosity and permeability in the ooid-oncoid-peloid grainstone facies. However, late diagenetic calcite and dolomite significantly altered porosity and permeability throughout the microbial thrombolite reservoir facies. Dolomite is restricted to the southwest portion of the microbial thrombolite reservoir, where blocky calcite occurs only in small amounts. The northeast portion of the reservoir has abundant coarse mosaic to blocky calcite cementation and local recrystallization of the calcite, but no dolomite. As the reservoir dips southwest, this heterogeneous cement distribution indicates that the deeper portion had a distinct pore water chemistry, different than the shallower northeast portion of the reservoir during late diagenesis.

Dolomitization is an important diagenetic process in changing pore system characteristics in LCCF. Dolomitization was associated with calcite dissolution, and resulted in changes in pore system geometry and enhancement of permeability. Dolomitization also created a more uniform vertical and lateral distribution of porosity and permeability in the microbial thrombolite facies.

Other Smackover Formation reservoirs, for example in Appleton and Vocation fields (Conecuh and Manila sub-basins,

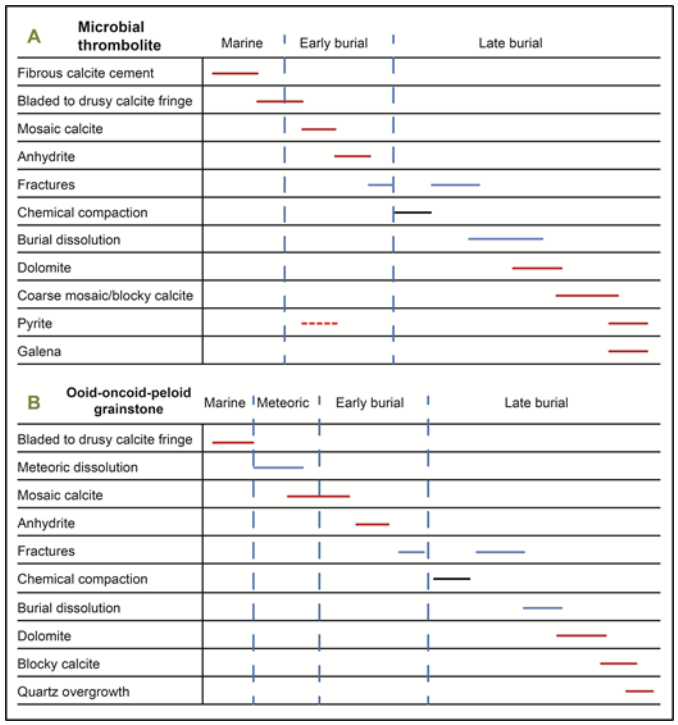

Figure 9. (A) Paragenetic evolution of the microbial thrombolite unit. (B) Paragenetic evolution of the ooid-oncoid-peloid grainstone unit. Events depicted as black lines destroyed or did not impact porosity; those depicted in blue enhanced porosity. Chemical compaction marks the boundary between early burial and late burial diagenesis. Uncertainty in the occurrence of events is indicated by the dashed line.

respectively [Fig. 1]) record extensive dolomitization that occurred in several steps: seawater-seepage, reflux, near-surface mixed-water, shallow-burial mixed-water, and deeper burial. The dolomites formed by these processes in Appleton and Vocation fields overlapped in time and space to form dolostone bodies composed of a complex mixture of dolomite types (Benson and Mancini, 1999; Prather, 1992b). In LCCF, only one dolomitization process occurred. The dolomite in LCCF has morphological and cathodoluminescence characteristics similar to those of the late rhombic dolomite cement in Appleton and Vocation fields, but it formed by a distinct process. In Appleton and Vocation fields, the rhombic dolomite is interpreted to be precompactional, shallow-burial mixed-water in origin (Prather, 1992b), but in LCCF it is interpreted to have formed in the deep burial environment. Trace-element composition of rhombic dolomites from LCCF and Appleton/Vocation fields are very different. The shallow-burial mixed-water dolomites in Appleton and Vocation fields have an average of 819 ppm of Na and 475 ppm of Sr (Prather, 1992b), whereas in the LCCF late burial dolomite these elements are absent. It is important to determine the origin and timing of the dolomitizing fluid to better characterize the reservoirs, to understand differences in petrophysical characteristics, and to predict similar reservoir characteristic in other fields. Appleton and Vocation fields have a different dolomite than LCCF, and the reservoir quality is affected by this difference. Appleton and Vocation thrombolitic reservoir units have higher mean porosity and permeability values, with a more homogeneous distribution of these petrophysical characteristics in the reservoir than in the thrombolitic reservoir of LCCF due to its intense early dolomitization process.

Good porosity and permeability in the Smackover Formation microbial thrombolite reservoir facies in LCCF also are related to late burial dissolution and fracturing, not dolomitization. Fluid percolation in the microbial thrombolite was more intense in the

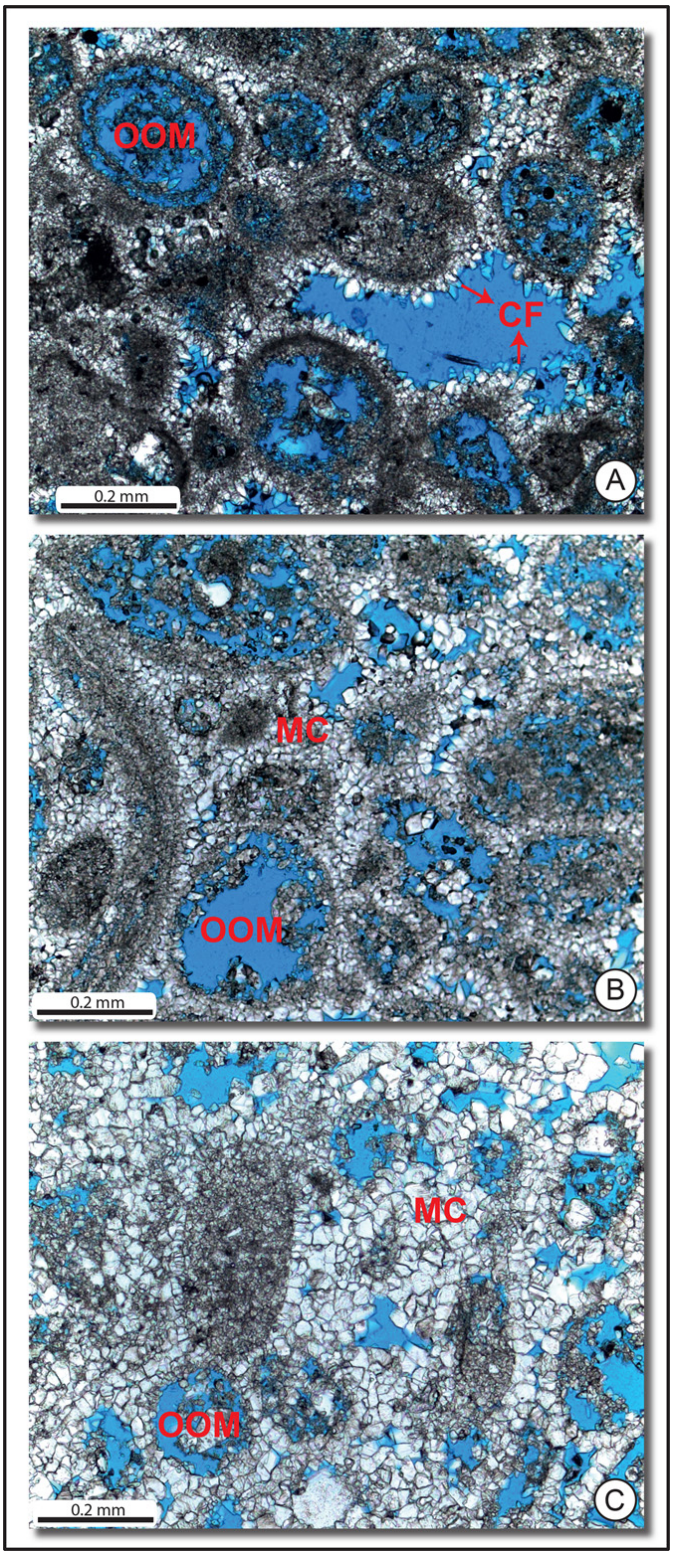

Figure 10. Photomicrographs illustrating degrees of diagenetic change in the ooid-oncoid-peloid grainstone, gradually increasing in intensity from A to C. (A) Partially dissolved ooids rimmed by bladed to drusy fringing calcite cement. Well 6—depth 11,346.2 ft. (B) Oomoldic grainstone with intergranular porosity mostly occluded by bladed to drusy fringing cement and fine mosaic calcite. Well 7—depth, 11,802.5 ft. (C) Oomoldic grainstone with intergranular porosity completely filled by coarse, mosaic calcite. Well 15—depth, 11,255.4 ft. CF, bladed to drusy calcite fringe cement; OOM, oomoldic porosity; and MC, fine mosaic calcite cement.

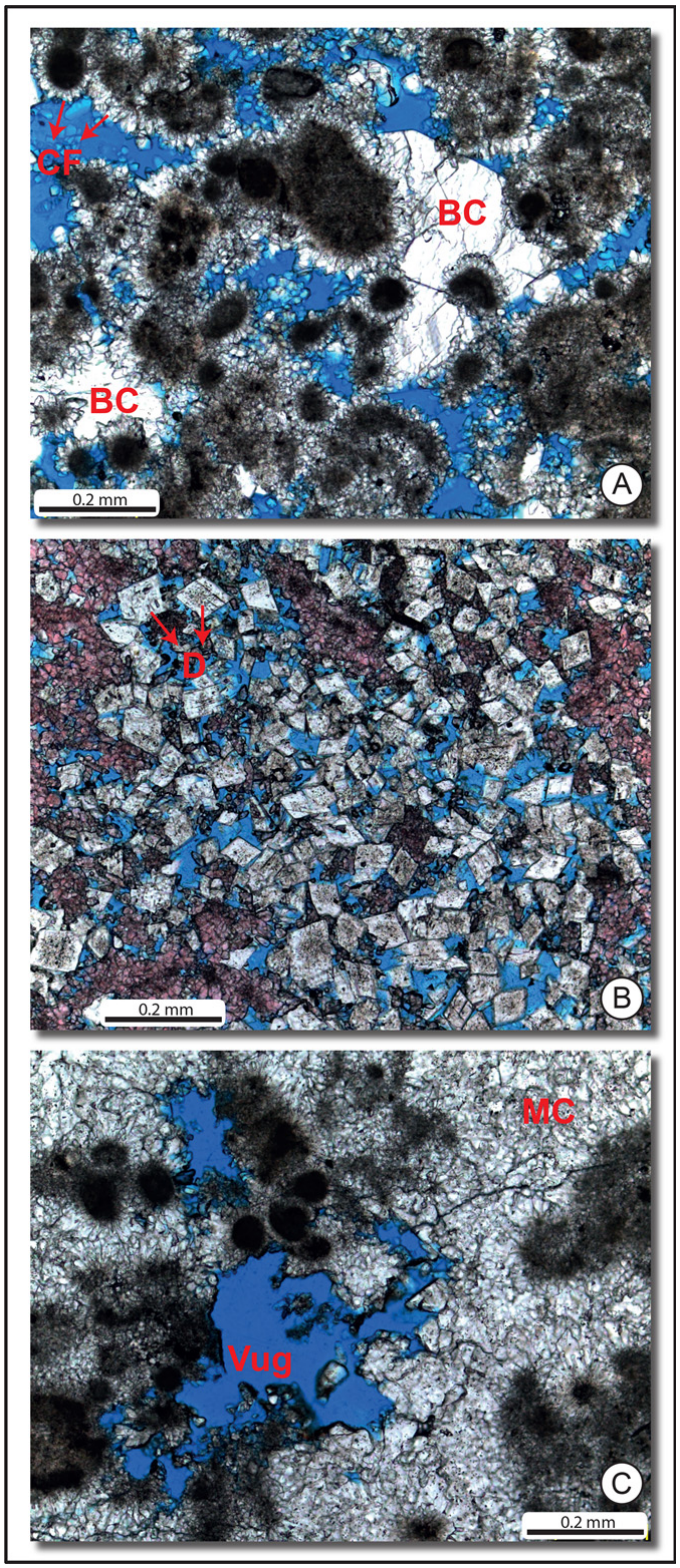

Figure 11. Photomicrographs of the microbial thrombolite facies. (A) Microbial peloids with fibrous calcite rims and blocky calcite partially cementing the pore space. Well 4—depth, 11,531.5 ft. (B) Intensely dolomitized microbial thrombolite. Well 2—depth, 11,789 ft. (C) Microbial thrombolite extensively cemented by mosaic calcite. Vuggy porosity created by late burial dissolution. Well 17—depth, 11,271.1 ft. CF, bladed to drusy calcite fringe cement; MC, fine mosaic calcite cement; BC, blocky calcite cement; D, dolomite; and Vug, vuggy pore type.

thicker portions of the bioherm, where a larger interval with good primary porosity and larger depositional constructional voids formed. Consequently, the largest secondary vugs, which can be as much as 2.4 in (6 cm) in diameter, occur in the areas where the microbial thrombolite is thicker. This process enhanced porosity and permeability in small, discontinuous intervals, and fractures also acted as conduits to fluid flow. The occurrence of large vugs intensely or completely cemented by calcite close to fractures, indicates dissolving and cementing fluids percolated through the fractures. Some stylolites also acted as local flow paths.

CONCLUSIONS

Lateral and vertical distribution of facies, cements, pore size, porosity, and permeability of the Smackover Formation in LCCF indicates that the reservoirs are controlled mainly by depositional facies, and secondarily by diagenesis, which caused significant changes in the pore system. The ooid-oncoid-peloid grainstone facies of LCCF can be subdivided in two sub-units: ooid grainstone and oncoid-peloid grainstone. These sub-units have distinct pore system geometry. The highest porosity values occur where the ooid-oncoid-peloid grainstone unit is thickest and where the ooid grainstone sub-unit dominates.

The ooid-oncoid-peloid grainstone and microbial thrombolite reservoirs facies were modified by a distinct early diagenetic process and similar late diagenetic evolution. The ooid-oncoid-peloid grainstone was exposed to meteoric waters, whereas the microbial thrombolite was not. Meteoric waters caused dissolution of the grains, generating secondary moldic porosity, and precipitation of drusy calcite fringe and very fine mosaic cement. The drusy calcite fringe blocked the pore throats, which significantly decreased permeability to 1 to 10 md. Late burial diagenetic processes were more intense in the microbial thrombolite facies. Dolomitization associated with calcite dissolution occurred in the south portion of the field, enhancing permeability and causing permeability values to be more uniform vertically and laterally. Late burial coarse mosaic to blocky calcite cementation was more intense in the north portion of the field, reducing primary porosity. Late burial dissolution process, which caused enlargement of depositional pores and created large vugs, was more intense in the thicker portions or the microbial thrombolite, and provided enhanced porosity and permeability.

ACKNOWLEDGMENTS

The authors are grateful to *Petrobras* (*Petróleo Brasileiro S/A*) for the financial support and providing access to the IMAGO® software, and to the Geological Survey of Alabama for access to the cores. We also thank Leslie Eliuk and Rick Major for their careful reviews of the manuscript.

REFERENCES CITED

Ahr, W. M., 1973, The carbonate ramp: An alternative to the shelf model: Gulf Coast Association of Geological Societies Transactions, v. 23, p. 221–225.

Ahr, W. M., and G. J. Palko, 1981, Depositional and diagenetic cycles in Smackover limestone-sandstone sequences, Lincoln Parish, Louisiana: Gulf Coast Association of Geological Societies Transactions, v. 31, p. 7–17.

Baria, L. R., D. L. Stoudt, P. M. Harris, and P. D. Crevello, 1982, Upper Jurassic reefs of Smackover Formation, United States Gulf Coast: American Association of Petroleum Geologists Bulletin, v. 66, p. 1449–1482.

Barret, M. L., 1986, Replacement geometry and fabrics of the Smackover (Jurassic) dolomite, southern Alabama: Gulf Coast Association of Geological Societies Transactions, v. 36, p. 9–18.

Benson, D. J., and E. A. Mancini, 1999, Diagenetic influence on reservoir development and quality in the Smackover updip basement ridge play, southwest Alabama: Gulf Coast Association of Geological Societies Transactions, v. 49, p. 96–101.

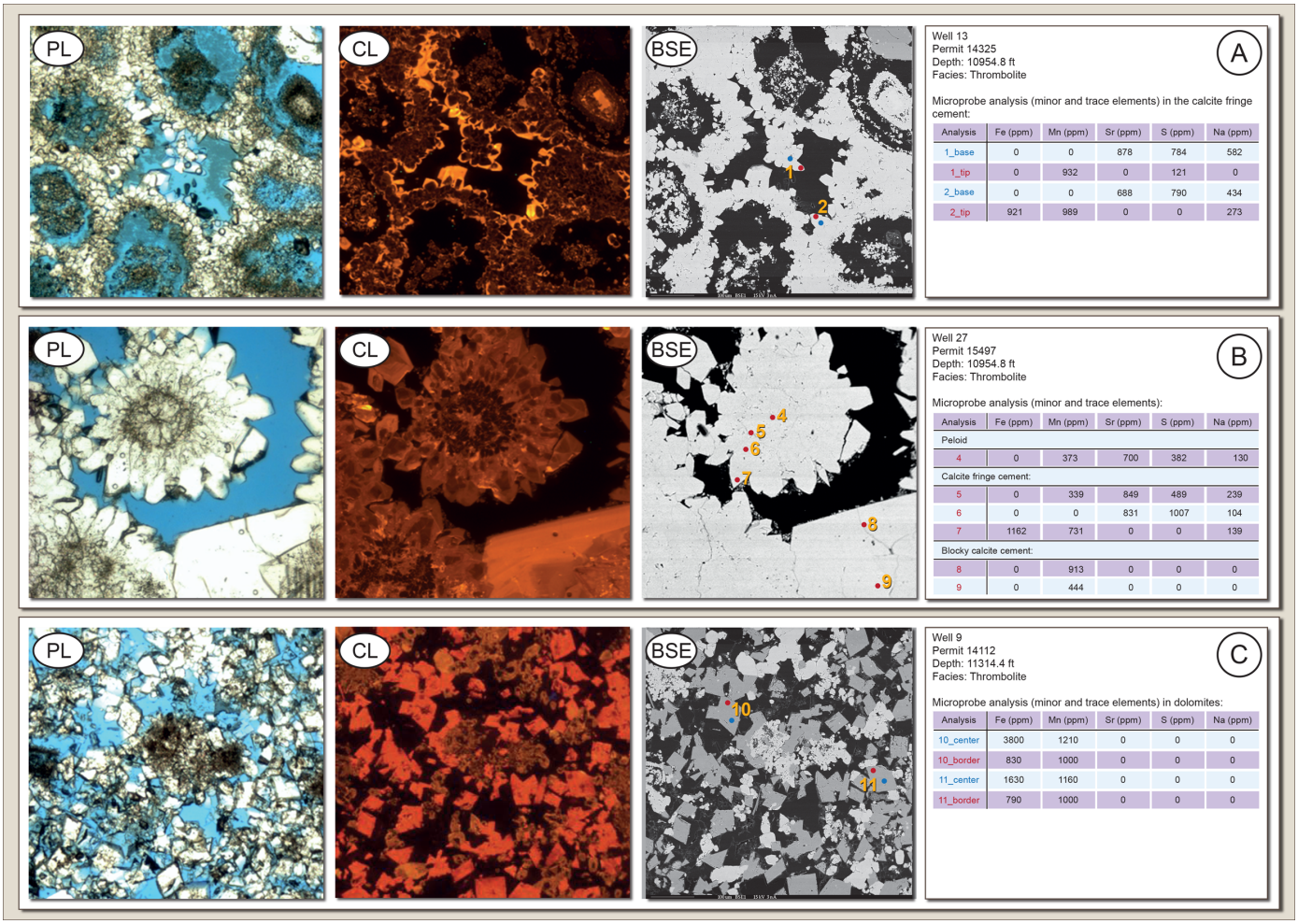

Figure 12. Plain light (PL) photomicrograph, cathodoluminescence (CL) image, and backscatter electron image (BSE) of (A) ooid-oncoid-peloid grainstone, (B) microbial thrombolite, and (C) partially dolomitized microbial thrombolite. Tables show microprobe analysis results (minor and trace elements). The exact points of the analyses are shown on the BSE images as colored dots. PL and CL images were taken after microprobe analysis, so it is possible to see the small holes (10 µm diameter) made by the microprobe electron beam. In (A), points 1 and 2 are bladed to drusy calcite fringing cement. In slide (B), point 4 is a microbial peloid, point 5 is fibrous calcite fringing cement, points 6 and 7 are drusy calcite fringing cement, and points 8 and 9 are blocky calcite cement. In slide (C), points 10 and 11 are rhombic dolomite.

Benson, J. D., 1988, Depositional history of the Smackover Formation in southwest Alabama: Gulf Coast Association of Geological Societies Transactions, v. 38, p. 197–205.

Budd, D. A., and L. S. Land, 1990, Geochemical imprint of meteoric diagenesis in Holocene ooid sands, Schooner Cays, Bahamas: Correlation of calcite cement geochemistry with extant groundwaters: Journal of Sedimentary Petrology, v. 60, p. 361–378.

Dickson, J. A. D., 1966. Carbonate identification and genesis as revealed by staining: Journal of Sedimentary Petrology, v. 36, p. 491–505.

Driskill, B. W., J. A. Nunn, R. Sassen, and R. H. Pilger, Jr., 1988, Tectonic subsidence, crustal thinning and petroleum generation in the Jurassic trend of Mississippi, Alabama and Florida: Gulf Coast Association of Geological Societies Transactions, v. 38, p. 257–265.

Dunham, R. J., 1962, Classification of carbonate rocks according to depositional texture: American Association of Petroleum Geologists, *in* W. E. Ham, ed., Classification of carbonate rocks—A symposium: American Association of Petroleum Geologists Memoir 1, Tulsa, Oklahoma, p. 108–121.

Kahle, C. F., 1965, Strontium in oolitic limestones: Journal of Sedimentary Petrology, v. 35, p. 846–856.

Kinsman, D. J. J., 1969, Interpretation of Sr^{+2} concentrations in carbonate minerals and rocks: Journal of Sedimentary Petrology, v. 39, p. 486–508.

Kopaska-Merkel, D. C., and S. D. Mann, 1991, Pore facies of Smackover carbonate reservoirs in southwest Alabama: Gulf Coast Association of Geological Societies Transactions, v. 41, p. 374–382.

Kopaska-Merkel, D. C., and S. D. Mann, 1993, Upward shoaling cycles in Smackover carbonates of southwest Alabama: Gulf Coast Association of Geological Societies Transactions, v. 43, p. 173–181.

Koralegadara, G., and W. C. Parcell, 2008, Reservoir characterization of microbial reef reservoirs at Little Cedar Creek Field, Conecuh County, Alabama: Proceedings of the 4th Annual GRASP Symposium, Wichita State University, Kansas, p. 57–58.

Llinas, J. C., 2002, Diagenetic history of the Upper Jurassic Smackover Formation and its effects on reservoir properties: Vocation Field, Manila Sub-basin, eastern Gulf Coastal Plain: Gulf Coast Association of Geological Societies Transactions, v. 52, p. 631–644.

Machel, H. G., 2000, Application of cathodoluminescence to carbonate diagenesis, *in* M. Pagel, V. Barbin, P. Blanc, and D. Ohnenstetter, eds., Cathodoluminescence in geosciences: Springer-Verlag, Berlin, Germany, p. 271–301.

Mancini, E. A., and D. J. Benson, 1980, Regional stratigraphy of Upper Jurassic Smackover carbonates of southwest Alabama: Gulf Coast Association of Geological Societies Transactions, v. 30, p. 151–165.

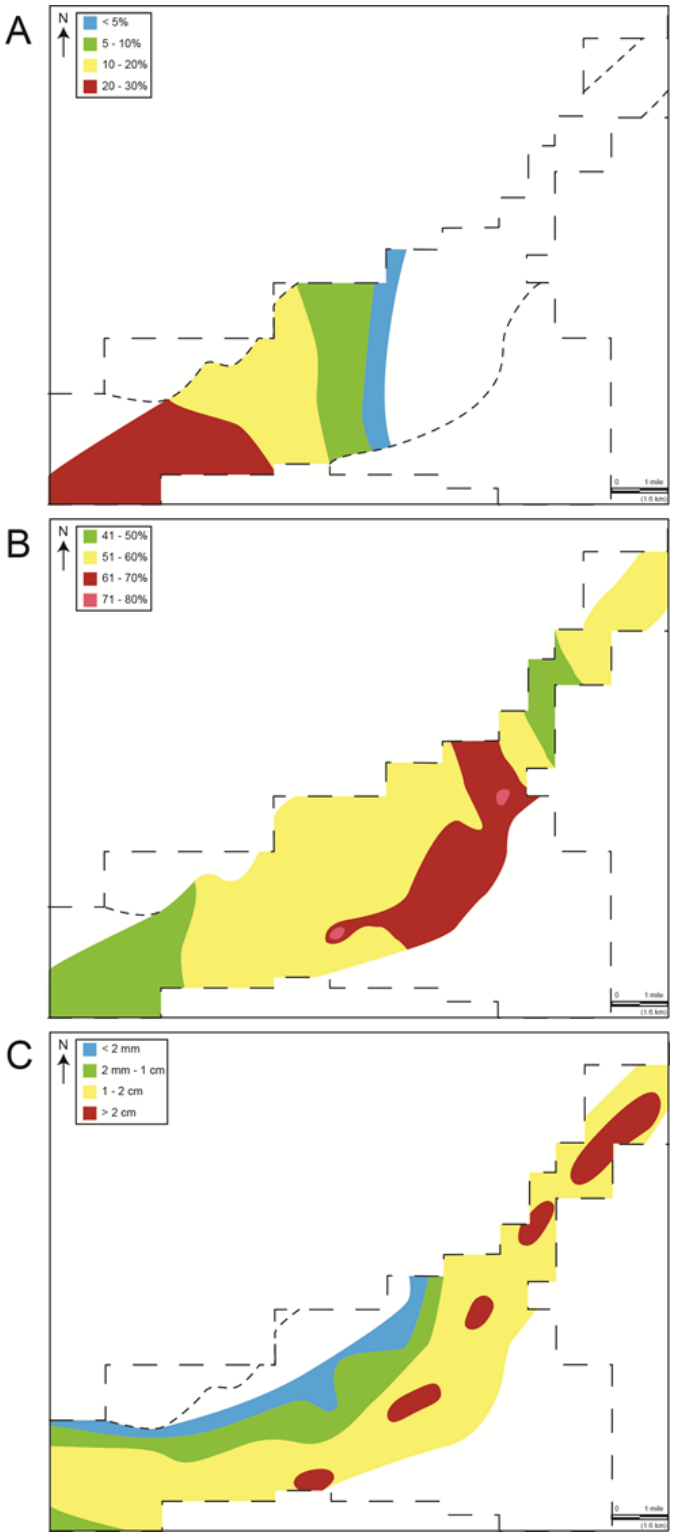

Figure 13. (A) Areal variation in dolomite content in the microbial thrombolite reservoir facies in LCCF. (B) Areal variation in cement (calcite and dolomite) in the microbial thrombolite reservoir facies in LCCF. (C) Lateral pore size variation in the microbial thrombolite reservoir facies in LCCF. See Figure 2A for map location.

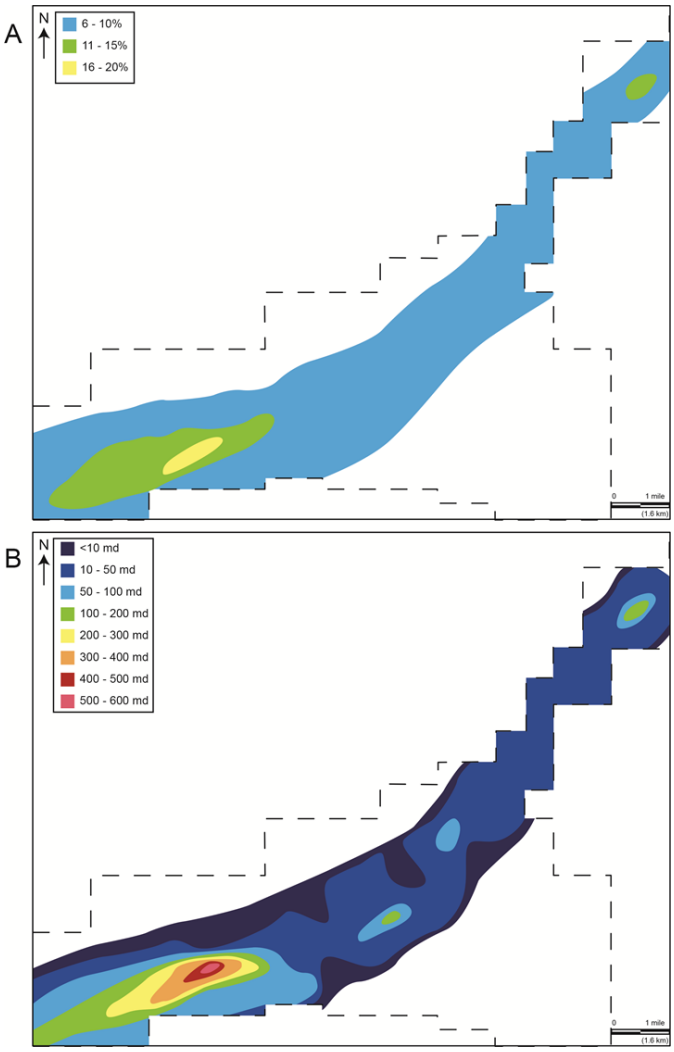

Figure 14. (A) Map of average porosity of the microbial thrombolite reservoir facies. (B) Map of the average permeability of the microbial thrombolite reservoir facies. See Figure 2A for map location.

Mancini, E. A., R. M. Mink, B. H. Tew, D. C. Kopaska-Merkel, and S. D. Mann, 1991, Upper Jurassic Smackover oil plays in Alabama, Mississippi and the Florida Panhandle: Gulf Coast Association of Geological Societies Transactions, v. 41, p. 475–480.

Mancini, E. A., W. C. Parcell, and W. M. Ahr, 2006, Upper Jurassic Smackover thrombolite buildups and associated nearshore facies, southwest Alabama: Gulf Coast Association of Geological Societies Transactions, v. 56, p. 551–563.

Mancini, E. A., W. C. Parcell, W. M. Ahr, V. O. Ramirez, J. C. Llinas, and M. Cameron, 2008, Upper Jurassic updip stratigraphic trap and associated Smackover microbial and nearshore carbonate facies, eastern Gulf Coastal Plain: American Association of Petroleum Geologists Bulletin, v. 92, p. 417–442.

Mancini, E. A., T. M. Puckett, and W. C. Parcell, 1999, Modeling of the burial and thermal histories of strata in the Mississippi Interior Salt Basin: Gulf Coast Association of Geological Societies Transactions, v. 49, p. 332–341.

Mancini, E. A., B. H. Tew, and R. M. Mink, 1990, Jurassic sequence stratigraphy in the Mississippi Interior Salt Basin of Alabama: Gulf Coast Association of Geological Societies Transactions, v. 40, p. 521–529.

Marshall, D. J., 1988, Cathodoluminescence of geological materials: Unwin Hyman, Boston, Massachusetts, 146 p.

Nunn, J. A., A. D. Scardina, and R. H. Pilger, 1984, Thermal evolution of the north-central Gulf Coast: Tectonics, v. 3, p. 723–740.

Parcell, W. C., 1999, Stratigraphic architecture of Upper Jurassic (Oxfordian) reefs in the northeastern U.S. Gulf Coast and the

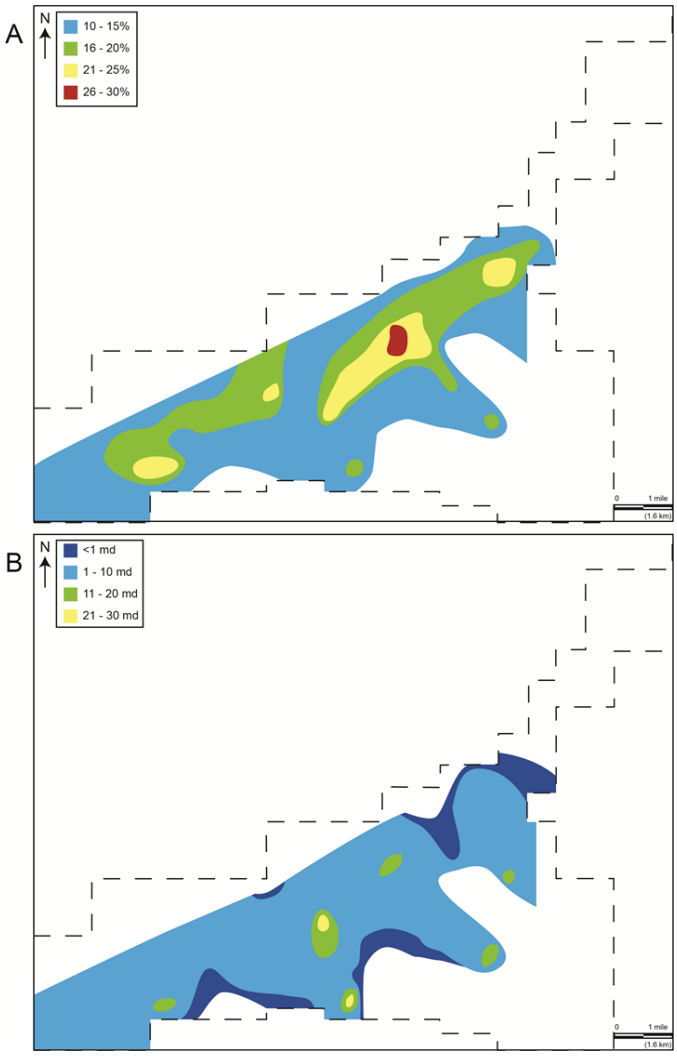

Figure 15. (A) Map of the average porosity of the ooid-oncoid-peloid grainstone reservoir facies. (B) Map of the average permeability of the ooid-oncoid-peloid grainstone reservoir facies. See Figure 2A for map location.

eastern Paris Basin, France: Gulf Coast Association of Geological Societies Transactions, v. 49, p. 412–417.

Petta, T. J., and S. D. Rapp, 1990, Appleton Field—U.S.A. Gulf of Mexico Basin, Alabama, *in* E. A. Beaumont and N. D. Foster, eds., Structural traps IV—Tectonic and nontectonic fold traps: American Association of Petroleum Geologists Atlas of Oil and Gas Fields and the Treatise of Petroleum Geology, Tulsa, Oklahoma, p. 299–318.

Prather, B. E., 1992a, Evolution of a Late Jurassic carbonate/evaporite platform, Conecuh Embayment, northeastern Gulf Coast, U.S.A.: American Association of Petroleum Geologists Bulletin, v. 76, p. 164–190.

Prather, B. E., 1992b, Origin of dolostone reservoir rocks, Smackover Formation (Oxfordian), northeastern Gulf Coast, U.S.A.: American Association of Petroleum Geologists Bulletin, v. 76, p. 133–163.

Richter, D. K., T. Goette, J. Goetze, and R. D. Neuser, 2003, Progress in application of cathodoluminescence (CL) in sedimentary petrology: Mineralogy and Petrology, v. 79, p. 127–166.

Salvador, A., 1987, Late Triassic-Jurassic paleogeography and origin of Gulf of Mexico Basin: American Association of Petroleum Geologists Bulletin, v. 71, p. 419–451.

Singh, U., 1987, Ooids and cements from the Late Precambrian of the Flinders Ranges, South Australia: Journal of sedimentary Petrology, v. 57, p. 117–127.

Williams, K. L., 1987, An introduction to x-ray spectrometry: X-ray fluorescence and electron microprobe analysis: Allen and Unwin, Sydney, Australia, 370 p.

APPENDIX

Table A–1. Effective reservoir thickness in core (ERTC), number of core plugs, and average values of porosity and permeability of each of the two reservoir units, and percentage of cement in the microbial thrombolite reservoir. Porosity cutoff values are 10% in the grainstone reservoir and 6% in the thrombolite reservoir.

		Thrombolite					Grainstone			
Well	API	ERTC (ft)	Num. of Plugs	Poro. (%)	Perm. (md)	Cement (%)	ERTC (ft)	Num. of Plugs	Poro. (%)	Perm. (md)
1	1035200770000	27.0	21	10	–	39	12.0	16	14	2.4
2	1035200880000	20.5	21	12	82.6	46	9.0	19	19	10.1
3	1035200910000	24.5	32	13	336.4	52	8.5	19	15	3.9
4	1035200940000	16.0	19	9	13.4	47	13.5	24	17	3.6
5	1035201020000	17.5	28	9	77.1	53	13.0	28	17	3.9
6	1035201050000	6.5	13	9	16.6	50	4.5	11	22	18.3
7	1035201080000	20.0	21	13	299.5	44	9.0	19	14	3
8	1035201100000	5.0	15	8	2.5	71	–	–	–	–
9	1035201110000	11.0	25	8	7.8	51	12.0	25	19	21.9
10	1035201130000	8.0	17	8	38.0	52	6.0	17	22	5.2
11	1035201190000	18.0	35	10	47.6	53	10.0	23	16	1.3
12	1035201210000	6.5	15	8	56.1	63	1.0	3	12	0.4
13	1035201220000	5.0	10	10	40.0	57	5.0	10	22	2.1
14	1035201260000	9.0	20	8	124.3	56	–	–	–	–
15	1035201280000	–	–	–	–	56	6.0	13	20	3.2
16	1035201290000	9.0	19	10	39.3	55	2.5	6	13	1.3
17	1035201390000	6.5	13	10	48.6	62	–	–	–	–
18	1035201400000	11.0	23	8	5.6	53	6.0	13	26	18.6
19	1035201430000	11.0	18	10	68.0	61	10.5	15	17	0.4
20	1035201440000	30.0	56	10	72.4	50	1.5	3	14	1.9
21	1035201470000	23.0	42	9	47.7	55	6.5	13	18	0.2
22	1035201500000	14.5	31	8	12.1	62	–	–	–	–
23	1035201530000	20.0	43	9	31.4	64	7.0	13	20	2.2
24	1035201560000	1.5	3	9	2.2	48	3.5	9	15	2.9
25	1035201590000	18.5	35	9	28.4	57	12.0	23	21	1.9
26	1035201600000	4.5	9	9	16.2	70	8.5	17	24	8.9
27	1035201610000	14.0	26	10	47.9	68	8.0	16	23	2.1
28	1035201720000	–	–	–	–	–	5.5	10	18	7.6
29	1035201870000	7.0	14	13	169.9	53	–	–	–	–
30	1035201960000	7.0	14	9	39.0	47	–	–	–	–
31	1035202000000	10.0	19	10	31.9	52	–	–	–	–
32	1035202090000	7.5	14	9	42.5	56	–	–	–	–

Table A–2. Effective reservoir thickness in core (ERTC), number of core plugs, and average values of porosity and permeability of the two reservoir facies. Porosity cutoff values are 10% in the grainstone reservoir and 6% in the thrombolite reservoir.

		Thrombolite				Grainstone			
Well	API	ERTC (ft)	Num. of Plugs	Poros. (%)	Perm. (md)	ERTC (ft)	Num. of Plugs	Poros. (%)	Perm. (md)
33	1035200900000	8.0	15	7	4.1	4.0	8	14	4.1
34	1035200920000	26.0	38	13	375.7	9.0	19	14	2.7
35	1035200960000	14.5	25	16	579.3	6.0	12	13	0.6
36	1035200980000	23.5	44	10	36.4	0.5	1	11	0.4
37	1035200990000	25.0	37	10	35.1	16.5	27	17	6.4
38	1035201010000	9.5	20	7	13.0	3.5	5	15	1.3
39	1035201040000	5.0	10	9	7.8	9.0	18	19	2.7
40	1035201060000	2.5	6	7	2.1	14.5	32	16	5.2
41	1035201070000	–	–	–	–	–	–	–	–
42	1035201140000	4.0	3	6	0.8	19.0	37	21	3.8
43	1035201150000	–	–	–	–	–	–	–	–
44	1035201160000	–	–	–	–	–	–	–	–
45	1035201170000	3.0	5	6	1.1	12.0	24	19	5.3
46	1035201180000	–	–	–	–	30.0	32	22	3.3
47	1035201200000	–	–	–	–	–	–	–	–
48	1035201230000	9.0	9	17	312.7	10.0	20	22	14.6
49	1035201240000	6.5	11	8	7.5	12.0	23	26	7.2
50	1035201250000	–	–	–	–	–	–	–	–
51	1035201270000	–	–	–	–	–	–	–	–
52	1035201300000	–	–	–	–	5.0	10	13	2.2
53	1035201310000	–	–	–	–	2.0	6	17	0.3
54	1035201340100	22.5	33	10	38.2	–	–	–	–
55	1035201360000	20.5	39	10	80.2	1.5	3	12	1.3
56	1035201380000	5.5	11	8	9.5	6.5	13	22	4.8
57	1035201410000	–	–	–	–	5.0	10	16	8.1
58	1035201420100	–	–	–	–	6.0	10	17	1.9
59	1035201460000	–	–	–	–	–	–	–	–
60	1035201550000	–	–	–	–	–	–	–	–
61	1035201580000	–	–	–	–	2.5	5	11	2.2
62	1035201620200	3.5	9	8	10.0	–	–	–	–
63	1035201640000	3.5	8	8	9.7	2.5	4	14	0.3
64	1035201660000	–	–	–	–	3.5	7	16	0.3
65	1035201700000	–	–	–	–	–	–	–	–
66	1035201740000	–	–	–	–	1.5	5	11	3.1
67	1035201750000	–	–	–	–	2.0	5	13	11.3
68	1035201760100	–	–	–	–	–	–	–	–
69	1035201790000	–	–	–	–	0.5	1	11	0.2
70	1035201800000	4.0	9	9	1.3	3.5	9	17	15.8
71	1035201820000	–	–	–	–	2.0	4	16	32.2
72	1035201850000	–	–	–	–	–	–	–	–
73	1035201890000	–	–	–	–	–	–	–	–
74	1035201910000	7.5	16	9	73.5	–	–	–	–
75	1035202020000	–	–	–	–	–	–	–	–
76	1035202050000	3.5	7	9	33.4	–	–	–	–
77	1035202100000	6.5	13	7	8.7	–	–	–	–

Table A–3. Microbial thrombolite microprobe analysis results.

		Ca (wt%)	Mg (wt%)	Fe (ppm)	Mn (ppm)	Sr (ppm)	S (ppm)	Na (ppm)
Peloid	**AVERAGE**	**39.50**	**0.37**	**304**	**384**	**737**	**391**	**215**
	Standard Deviation	0.39	0.08	0	132	98	112	48
	Range	38.96/39.89	0.24/0.49	0	282/660	617/837	210/580	130/299
	Analysis	**10**	**10**	1	**8**	4	**10**	**8**
	Analysis below LLD	0	0	**9**	2	**6**	0	2
Fibrous calcite fringe	**AVERAGE**	**39.58**	**0.40**	**0**	**508**	**849**	**455**	**221**
	Standard Deviation	0.26	0.08	0	311	0	141	48
	Range	39.24/39.83	0.30/0.50	0	315/970	0	205/616	148/282
	Analysis	**6**	**6**	0	**4**	1	**6**	**6**
	Analysis below LLD	0	0	**6**	2	**5**	0	0
Drusy calcite fringe (all analyses))	AVERAGE	**39.71**	**0.31**	**0**	**806**	**693**	**476**	**207**
	Standard Deviation	0.31	0.16	0	795	97	243	64
	Range	39.05/40.29	0.05/0.68	0	320/3570	617/831	165/1007	122/334
	Analysis	**27**	**27**	0	**15**	5	**17**	12
	Analysis below LLD	0	0	**26**	12	**22**	10	**15**
Drusy calcite fringe fringe base	AVERAGE	**39.65**	**0.39**	**0**	**502**	**748**	**499**	**237**
	Standard Deviation	0.23	0.09	0	232	111	215	58
	Range	39.29/39.96	0.23/0.54	0	315/970	617/849	205/1007	148/334
	Analysis	**9**	**9**	0	4	3	**8**	4
	Analysis below LLD	0	0	**9**	**5**	**6**	1	**5**
Drusy calcite fringe fringe tip	AVERAGE	**39.90**	**0.20**	**0**	**705**	**0**	**339**	**167**
	Standard Deviation	0.34	0.13	0	299	0	143	40
	Range	39.38/40.29	0.05/0.47	0	507/1281	0	183/465	139/195
	Analysis	**9**	**9**	0	**6**	0	3	2
	Analysis below LLD	0	0	**8**	3	**9**	**6**	**7**
Mosaic calcite	AVERAGE	**40.17**	**0.22**	**0**	**942**	**935**	**213**	**152**
	Standard Deviation	0.27	0.11	0	489	13	96	18
	Range	39.83/40.54	0.05/0.46	0	954/2985	926/944	194/412	159/165
	Analysis	**20**	**20**	0	**20**	2	8	2
	Analysis below LLD	0	0	**8**	0	**18**	**12**	**18**
Blocky calcite	AVERAGE	**40.11**	**0.20**	**809**	**821**	**0**	**166**	**159**
	Standard Deviation	0.31	0.09	380	258	0	97	42
	Range	39.53/40.07	0.03/0.33	400/1432	339/2070	0	124/237	130/221
	Analysis	**32**	**32**	10	**30**	0	3	4
	Analysis below LLD	0	0	**22**	2	**32**	**29**	**28**
Dolomite (all analyses)	AVERAGE	**22.62**	**12.63**	**2336**	**1157**	**0**	**0**	**210**
	Standard Deviation	0.20	0.21	2131	187	0	0	0
	Range	22.31/22.87	12.35/12.88	790/6520	980/1500	0	0	0
	Analysis	**7**	**7**	**7**	**7**	0	0	1
	Analysis below LLD	0	0	0	0	**7**	**7**	**1**
Dolomite center	AVERAGE	**22.54**	**12.62**	**2083**	**1117**	**0**	**0**	**0**
	Standard Deviation	0.29	0.24	1541	121	0	0	0
	Range	22.31/22.87	12.35/12.81	820/3800	980/1210	0	0	0
	Analysis	**3**	**3**	**3**	**3**	0	0	0
	Analysis below LLD	0	0	0	0	**3**	**3**	**3**
Dolomite border	AVERAGE	**22.70**	**12.49**	**4240**	**1375**	**0**	**0**	**210**
	Standard Deviation	0.10	0.19	3224	177	0	0	0
	Range	22.63/22.77	12.35/12.62	1960/6520	1250/1500	0	0	0
	Analysis	**2**	**2**	**2**	**2**	0	0	1
	Analysis below LLD	0	0	0	0	**2**	**2**	**1**

Practical Lower Limit of Detection (LLD)						
Ca (wt%)	Mg (wt%)	Fe (ppm)	Mn (ppm)	Sr (ppm)	S (ppm)	Na (ppm)
0.034	0.021	300	260	580	120	120

Table A–4. Ooid-oncoid-peloid grainstone microprobe analysis results.

		Ca (wt%)	Mg (wt%)	Fe (ppm)	Mn (ppm)	Sr (ppm)	S (ppm)	Na (ppm)
Oolite	**AVERAGE**	**40.13**	**0.27**	**458**	**0**	**2704**	**606**	**309**
	Standard Deviation	**0.33**	**0.15**	**95**	**0**	**1559**	**257**	**112**
	Range	**39.57/40.58**	**0.10/0.53**	**390/525**	**0**	**748/4807**	**313/928**	**182/421**
	Analysis	**6**	**6**	**2**	**0**	**6**	**6**	**5**
	Analysis below LLD	**0**	**0**	**4**	**6**	**0**	**0**	**1**
Bladed to drusy calcite fringe (all analyses)	**AVERAGE**	**39.73**	**0.30**	**731**	**740**	**722**	**570**	**318**
	Standard Deviation	0.20	0.14	284	294	97	237	124
	Range	39.41/40.04	0.10/0.56	405/921	378/989	623/878	121/924	174/582
	Analysis	**18**	**18**	3	4	8	**13**	**10**
	Analysis below LLD	0	0	**15**	**14**	**10**	5	8
Bladed to drusy calcite fringe crystal base	**AVERAGE**	**39.73**	**0.35**	**0**	**0**	**755**	**649**	**378**
	Standard Deviation	0.23	0.15	0	0	90	238	126
	Range	39.43/40.04	0.11/0.56	0	0	641/878	252/924	239/582
	Analysis	**8**	**8**	**0**	**0**	**6**	**7**	**6**
	Analysis below LLD	0	0	8	8	2	1	2
Bladed to drusy calcite fringe crystal tip	**AVERAGE**	**39.73**	**0.26**	**663**	**795**	**623**	**477**	**229**
	Standard Deviation	0.22	0.12	365	288	0	220	41
	Range	39.41/39.97	0.10/0.46	405/921	464/989	623	121/806	0/273
	Analysis	**8**	**8**	2	3	**2**	**6**	**4**
	Analysis below LLD	0	0	**6**	**5**	0	2	4
Mosaic calcite	**AVERAGE**	**39.07**	**0.17**	**353**	**272**	**4121**	**496**	**476**
	Standard Deviation	2.65	0.17	**38**	**0**	1598	236	171
	Range	32.14/40.74	0.06/0.66	**323/424**	**0**	599/6796	226/1046	182/1007
	Analysis	**24**	**24**	**7**	**1**	**24**	**21**	**22**
	Analysis below LLD	0	0	**17**	**23**	0	3	2
Blocky calcite	AVERAGE	**39.72**	**0.19**	**755**	**863**	**0**	**0**	**156**
	Standard Deviation	0.44	0.01	99	192	0	0	0
	Range	38.65/40.17	0.18/0.22	598/916	574/1147	0	0	0
	Analysis	**11**	**11**	**11**	**11**	0	0	1
	Analysis below LLD	0	0	0	0	**11**	**11**	**10**
Dolomite	AVERAGE	**22.52**	**12.75**	**1167**	**1080**	**0**	**0**	**150**
	Standard Deviation	0.10	0.06	133	121	0	0	0
	Range	22.48/22.63	12.70/12.81	1090/1320	950/1190	0	0	0
	Analysis	**3**	**3**	**3**	**3**	0	0	1
	Analysis below LLD	0	0	0	0	**3**	**3**	**2**

Practical Lower Limit of Detection (LLD)

Ca (wt%)	Mg (wt%)	Fe (ppm)	Mn (ppm)	Sr (ppm)	S (ppm)	Na (ppm)
0.034	0.021	300	260	580	120	120